GASTROENTEROLOGY 2001;120:1620–1629

Fluorescence, Reflectance, and Light-Scattering Spectroscopy for Evaluating Dysplasia in Patients With Barrett's Esophagus

IRENE GEORGAKOUDI,* BRIAN C. JACOBSON,† JACQUES VAN DAM,† VADIM BACKMAN,* MICHAEL B. WALLACE,§ MARKUS G. MÜLLER,* QINGGUO ZHANG,* KAMRAN BADIZADEGAN,‖ DON SUN,¶ GORDON A. THOMAS,* LEV T. PERELMAN,* and MICHAEL S. FELD*

*G.R. Harrison Spectroscopy Laboratory, Massachusetts Institute of Technology, Cambridge, Massachusetts; †Division of Gastroenterology, Department of Medicine, Brigham & Women's Hospital, Harvard Medical School, Boston, Massachusetts; §Digestive Disease Center, Medical University of South Carolina, Charleston, South Carolina; ‖Department of Pathology, Children's Hospital, Harvard Medical School, Boston, Massachusetts; ¶Statistics Department, Lucent Technologies, Inc., Bell Laboratories, Murray Hill, New Jersey

Background & Aims: **The aim of this study was to assess the potential of 3 spectroscopic techniques (fluorescence, reflectance, and light-scattering spectroscopy) individually and in combination, for evaluating low- and high-grade dysplasia in patients with Barrett's esophagus (BE).** ***Methods:*** **Fluorescence spectra at 11 excitation wavelengths and a reflectance spectrum were acquired in approximately 1 second from each site before biopsy using an optical fiber probe. The measured fluorescence spectra were combined with the reflectance spectra to extract the intrinsic tissue fluorescence. The reflectance spectra provided morphologic information about the bulk tissue, whereas light-scattering spectroscopy was used to determine cell nuclear crowding and enlargement in Barrett's epithelium.** ***Results:*** **Significant differences were observed between dysplastic and nondysplastic BE in terms of intrinsic fluorescence, bulk scattering properties, and levels of epithelial cell nuclear crowding and enlargement. The combination of all 3 techniques resulted in superior sensitivity and specificity for separating high-grade from non–high-grade and dysplastic from nondysplastic epithelium.** ***Conclusions:*** **Intrinsic fluorescence, reflectance, and light-scattering spectroscopies provide complementary information about biochemical and morphologic changes that occur during the development of dysplasia. The combination of these techniques (Tri-Modal Spectroscopy) can serve as an excellent tool for the evaluation of dysplasia in BE.**

Adenocarcinoma of the lower esophagus develops almost exclusively in patients with Barrett's esophagus (BE), a condition characterized by the presence of metaplastic columnar epithelium.[1] Although the prognosis of patients diagnosed with adenocarcinoma is poor, the chances of successful treatment increase significantly if the disease is detected at the dysplastic stage.[2] The surveillance of patients with BE for dysplasia is challenging in 2 respects. First, dysplasia is not visible during routine endoscopy.[3] Thus, numerous random biopsy specimens are required. Second, the histopathologic diagnosis of dysplasia is problematic because there is poor interobserver agreement on the classification of a particular specimen, even among expert gastrointestinal pathologists.[4,5]

Optical techniques, such as fluorescence,[6–13] reflectance, and light-scattering[14] spectroscopies or optical coherence tomography[15–18] may significantly enhance the endoscopist's ability to detect these early dysplastic changes in BE. Indeed, fluorescence spectroscopy studies using exogenous fluorophores, such as Photofrin (QLT, Vancouver, Canada) and aminolevulinic acid–induced protoporphyrin IX, show that there is a significant difference between the measured red fluorescence of the carcinomatous and nondysplastic tissue as a result of the preferential accumulation of the drug.[10–13] Initial autofluorescence spectroscopy studies performed at 410 nm excitation report promising results for detecting high-grade dysplasia.[6–9] However, focal high-grade and low-grade lesions could not be detected reliably.

The aim of this study is to show that a combination of spectroscopic techniques can improve the sensitivity and accuracy of dysplasia detection in patients with BE. We show that fluorescence, reflectance, and light-scattering spectroscopies provide complementary information about the biochemical, architectural, and morphologic state of tissue and the corresponding changes that occur during the progression of dysplasia.

The need for using reflected light to correct for the effects of hemoglobin absorption on the measured integrated tissue fluorescence intensity has been recognized

Abbreviations used in this paper: BE, Barrett's esophagus; EEM, excitation-emission matrix; LSS, light-scattering spectroscopy; NADH, reduced nicotinamide adenine dinucleotide; PC, principal component.

0016-5085/01/$35.00
doi:10.1053/gast.2001.24842

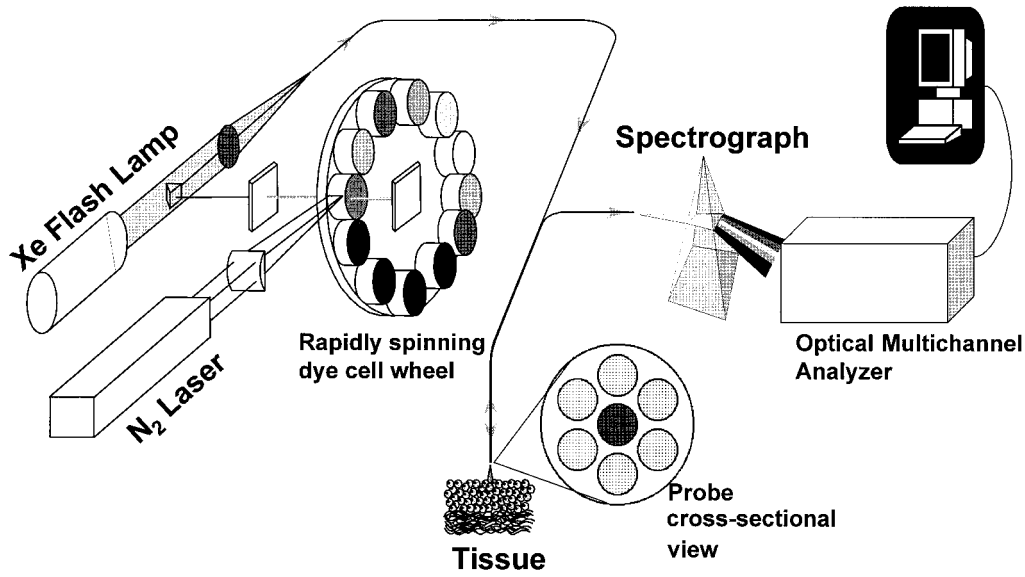

Figure 1. Schematic of fast EEM instrument. During endoscopy, the probe was inserted into the accessory channel of the endoscope and brought into gentle contact with the tissue, thus providing a fixed delivery-collection geometry. The reflected and fluorescence light was collected by the probe and coupled to a spectrograph and detector. The average of 3 sets of spectra from each site was used for analysis. Immediately after spectral acquisition, the probe was removed and a slight demarcation remained on the tissue for 30–60 seconds as a result of the probe contact. This endoscopically apparent marker was used as a guide for taking a biopsy specimen from the same site at which spectra were acquired. The biopsy specimen was interpreted and classified by an experienced gastrointestinal pathologist. If a dysplastic lesion was suspected, the specimen was reviewed and the diagnosis confirmed by a second gastrointestinal pathologist, in accordance with the standard of care. Data were analyzed from 26 nondysplastic BE sites (9 patients), 7 low-grade (4 patients), and 7 high-grade (5 patients) dysplastic sites.

and implemented by several groups in animal studies.[19–21] We illustrate, for the first time to our knowledge in a clinical setting, how the combination of fluorescence and reflectance spectroscopies can be applied to remove distortions introduced by scattering and absorption into the entire measured tissue fluorescence spectrum. The undistorted fluorescence can serve as a sensitive indicator of tissue biochemistry, whereas reflectance and light-scattering spectroscopies provide morphologic information on tissue architecture and epithelial cell nuclei. This is the first report of the simultaneous use of all 3 spectroscopic techniques for characterizing tissue and diagnosing disease. Our results show that the combined use of all 3 techniques (Tri-Modal Spectroscopy) provides superior results compared with the results of each technique individually, in terms of detecting not only high-grade, but also low-grade, dysplastic changes in BE.

Materials and Methods

The study was conducted at the Brigham and Women's Hospital and the West Roxbury Veterans Administration Medical Center. The protocol was approved by the Institutional Review Boards of both hospitals, as well as by the Committee On the Use of Humans as Experimental Subjects of the Massachusetts Institute of Technology. Data were collected from 16 patients with known BE undergoing standard surveillance protocols.

Measurements were performed using a fast excitation-emission matrix (EEM) instrument developed in our laboratory.[22] The excitation light source of this fast EEM system consisted of a 337-nm nitrogen laser (model VSL-337MD; Laser Science, Inc., Franklin, MA) pumping 10 dye cuvettes precisely mounted on a rapidly rotating wheel. In this manner, 11 different excitation wavelengths were obtained between 337 and 620 nm and coupled into the delivery fiber of a 1-mm diameter optical fiber probe. For the reflectance measurements, white light (350–700 nm) from a Xe flash lamp (Perkin Elmer Optoelectronics, Salem, MA) was coupled into the same probe. The probe was composed of 6 collection fibers surrounding the central light delivery fiber, and it was covered with a protective, transparent optical shield[23] (Figure 1).

Three types of spectroscopic information were acquired in less than 1 second. Fluorescence spectra at 11 different excitation wavelengths, reflectance spectra, and light-scattering spectra were obtained. Each type of spectrum was analyzed in a manner that provided information about biochemical and morphologic changes that occur during dysplastic transformation.

Fluorescence spectroscopy can provide valuable information about changes that take place in tissue biochemistry during the development of dysplasia. However, the measured tissue fluorescence spectra can be distorted significantly by unrelated scattering and absorption events. To remove these distortions, the fluorescence spectra were analyzed in combination with information from the corresponding reflectance spectra.[24,25] The success of this simple model is predicated on the fact that fluorescence and reflectance spectra collected from a specific

site using the same light delivery/collection geometry undergo similar distortions. By extracting the intrinsic (undistorted) tissue fluorescence, changes in tissue biochemistry were isolated in a more sensitive and specific manner.

Principal component (PC) analysis[26] and logistic regression[27,28] were used to determine the correlation between spectral features of the intrinsic fluorescence and histopathologic diagnosis. PC analysis is a statistical tool that generates a minimal set of basis spectra (PCs) from an experimental data set. These PCs can be combined linearly to describe accurately the experimental spectra. PCs are numbered in a manner that corresponds to the amount of variance they represent in the data. Thus, the first PC accounts for the spectral features that vary the most, and subsequent PCs represent features with progressively smaller variance. Usually, only a relatively small number of PCs are required to fit the spectra to within the accuracy of the noise. Only PCs that described meaningful and significant spectral changes were included in the second step of our statistical analysis.

To analyze this relatively small data set in an unbiased manner, leave-one-out cross-validation[29,30] was used. Specifically, the PCs of the intrinsic fluorescence spectra that described the spectral features that change during the progression of dysplasia were selected. The corresponding scores (the coefficients describing the contributions of the principal components to the overall spectra) were used to determine our ability to distinguish (1) high-grade dysplasia from low-grade dysplastic and nondysplastic BE, and (2) dysplastic (low- and high-grade) from nondysplastic BE. To achieve that in an unbiased manner, the following cross-validation procedure was performed. The scores from a particular site were eliminated, and logistic regression was used to form a decision surface that classified the remaining sites in a manner that optimized agreement with the histopathological classification. The resulting decision surface was then used to classify the excluded site. This process was repeated for each of the sites. This method, known as leave-one-out or jackknife cross-validation, provided optimal use of a relatively small data set to validate the performance of a decision surface without bias.[29,30] The decision surface varied minimally during this procedure, indicating the robustness of the technique. Sensitivity and specificity values were determined by comparing the spectroscopic classification with histopathology. Statistical analysis was performed using Matlab statistics software (The MathWorks, Inc., Natick, MA).

The measured reflectance spectra were analyzed using a model based on a diffusion theory, which expressed the reflected light as a function of the absorption (μ_a) and reduced scattering (μ_s') coefficients of tissue.[31] This analysis provided information about the architecture and morphology of mainly the connective tissue,[32] i.e., the lamina propria and the submucosa, because the collected light originated within 500–700 μm from the tissue surface and the epithelium in Barrett's esophagus consists mainly of a single cell layer. A linear fit was performed to describe the wavelength dependence of μ_s'. The diagnostic value of the slope and intercept of this line was determined by correlating the results of logistic regression and cross-validation with histopathological classification, as in the intrinsic fluorescence case.

Light-scattering spectroscopy (LSS) was used to characterize the epithelial cell nuclei.[33,34] LSS spectra were extracted from the reflectance data by subtracting the diffuse component provided by the model of Zonios et al.[31] The LSS signal comprised a small fraction of the reflected light and was caused by photons that were singly backscattered by the cell nuclei. The intensity of the LSS spectrum varied in wavelength in an oscillatory manner. The frequency of these oscillations are proportional to the size of the scatterers (cell nuclei), and the depth of the modulations is proportional to the density of the scatterers, which in this case is indicative of nuclear crowding.[33] These variations were analyzed using a model based on the theory of light scattering to determine the number and size of the epithelial cell nuclei.[33] Logistic regression and cross-validation were then used to compare the spectroscopic classification with that of histopathology. To optimize sensitivity and specificity, the posterior probability threshold for separating high-grade dysplasia from non–high-grade dysplasia sites was set to 0.3.

Finally, results from all 3 spectroscopic techniques were combined to determine whether the number of correctly classified sites could be improved. Specifically, a site was assigned a classification that was consistent with the results from at least 2 of the 3 analysis methods, and this classification was compared with histopathology.

Results

Extracting the Intrinsic Tissue Fluorescence

Figure 2*A* shows a typical fluorescence spectrum excited with 337 nm light from a nondysplastic BE site (solid line). There are 2 peaks, which might be attributed to the presence of 2 different tissue fluorophores. However, note that the fluorescence intensity decrease between these 2 peaks occurs in the 420-nm wavelength range, where hemoglobin absorbs light very efficiently. The effects of hemoglobin absorption are clearly observed in the corresponding reflectance spectrum, which exhibits minima at approximately 420, 540, and 580 nm, corresponding to oxyhemoglobin absorption peaks (Figure 2*B*).

When the measured fluorescence spectrum of Figure 2*A* is processed in combination with the corresponding reflectance spectrum of Figure 2*B* as discussed in Materials and Methods, the intrinsic (undistorted) tissue fluorescence spectrum at the particular excitation wavelength is obtained (Figure 2*A*, dashed line). Note that this spectrum consists of a single broad peak.

Significant differences are observed in the modeled intrinsic tissue fluorescence of nondysplastic and dysplastic BE sites excited at 337 nm (Figure 3*A* and *B*) and 397

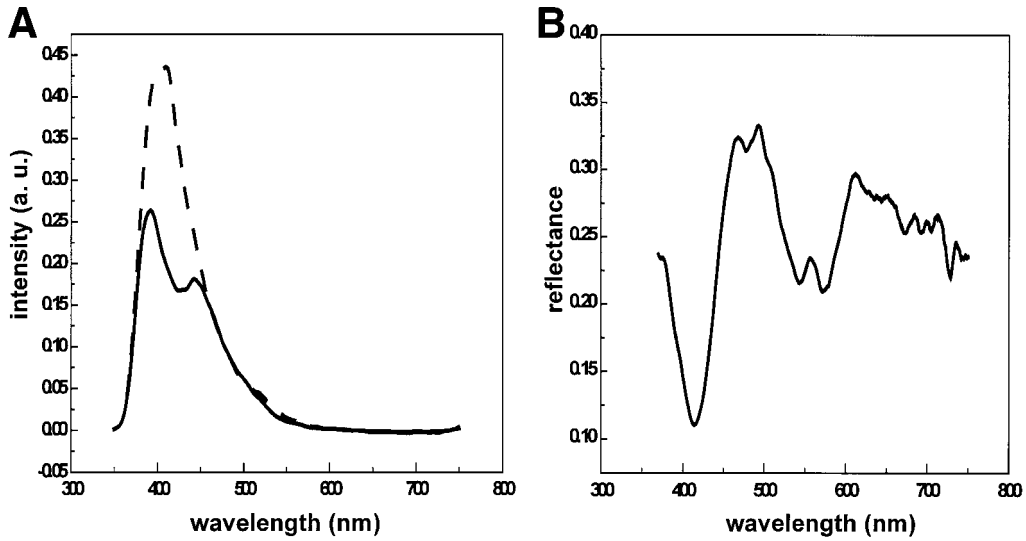

Figure 2. (*A*) Fluorescence from a nondysplastic BE site, 337-nm excitation. Measured spectrum, solid line; extracted intrinsic fluorescence, dashed line. (*B*) Corresponding reflectance spectrum.

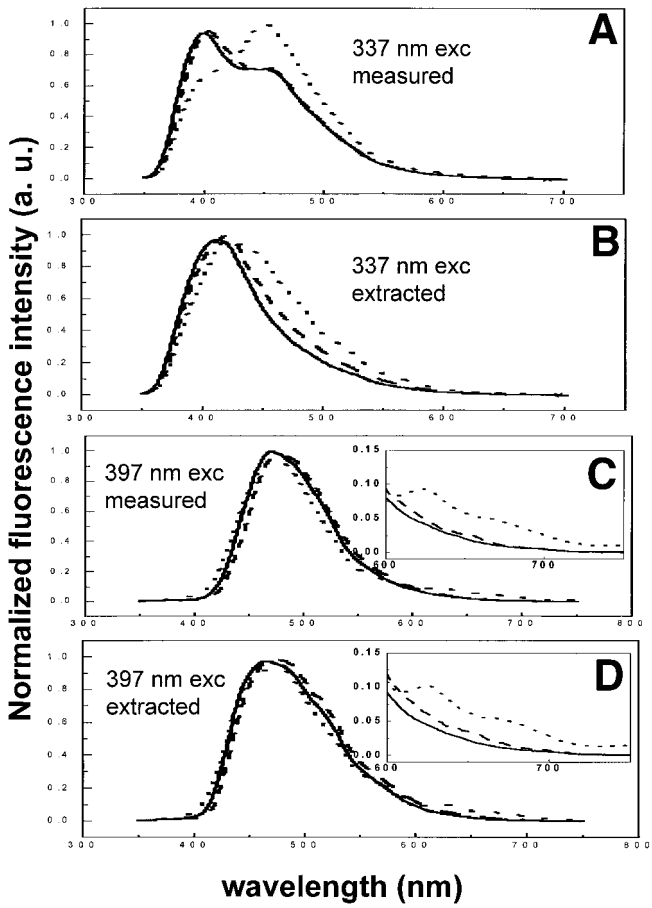

Figure 3. Mean fluorescence spectra from nondysplastic (*solid lines*), low-grade (*dashed lines*), and high-grade dysplastic (*dotted lines*) BE sites. Measured and corresponding extracted intrinsic fluorescence for excitation at 337 nm and 397 nm are shown. The insets in (*C*) and (*D*) show a magnified view of the corresponding spectra in the 600–750-nm region. Spectra are normalized to their peak intensities. Note the significant line-shape changes.

nm (Figure 3*C* and *D*). At 337-nm excitation, the lineshape of the dysplastic sites broadens and shifts to the red region of the spectrum during the progression from nondysplastic, to low-grade, to high-grade dysplasia. At 397-nm excitation, the fluorescence increases in the red region of the spectrum for the dysplastic BE sites. Similar changes are observed at 412-nm excitation (data not shown).

These differences can be exploited to develop algorithms for detecting dysplasia in BE. Specifically, principal component analysis, logistic regression, and leave-one-out cross-validation are used to determine the sensitivity and specificity with which we can separate (1) nondysplastic from dysplastic (low- and high-grade) tissue, and (2) high-grade dysplasia from low-grade and nondysplastic BE epithelium. In each case, the scores of 1 of the first 2 principal components extracted from the intrinsic fluorescence spectra at 337-, 397-, and 412-nm excitation are used (Figures 4 and 5). The selected principal components describe the observed spectral differences already discussed. From this analysis, sites with high-grade dysplasia can be differentiated from low-grade and nondysplastic sites with high levels of sensitivity and specificity (Table 1). Additionally, dysplastic and nondysplastic epithelia can be distinguished with very high sensitivity and specificity (Table 1).

Reflectance Spectroscopy

As discussed in Materials and Methods, the reflectance spectra can be analyzed using a mathematical model to obtain detailed information about the scattering and absorption properties of the bulk tissue. A typical reflectance spectrum with the corresponding fit obtained using this model is shown in Figure 6.

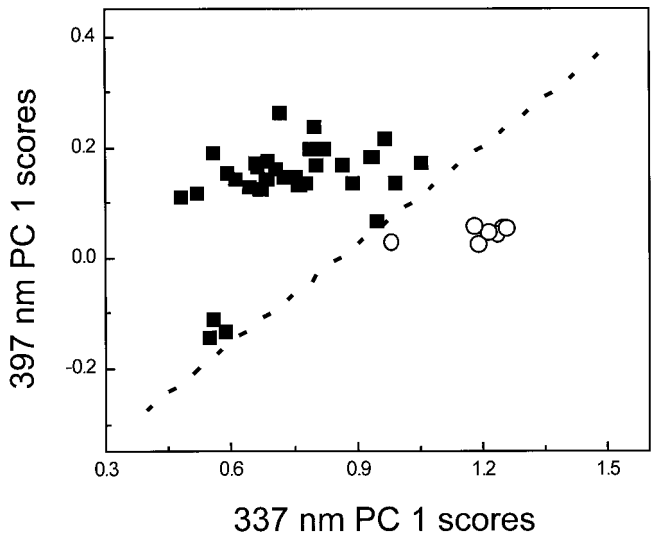

Figure 4. Scores of 2 principal components extracted from decomposition of intrinsic fluorescence spectra at 337- and 397-nm excitation used to distinguish high-grade dysplasia (○) from nondysplastic and low-grade dysplasia (■) BE sites. At 337-nm excitation, decomposition was performed in the 460–520-nm region of the intrinsic fluorescence spectra because this is the wavelength range within which spectral differences are most pronounced. Similarly, at 397-nm excitation, principal components were extracted from the intrinsic fluorescence spectra between 600 and 650 nm. PC 1, first principal component. The dotted line represents the logistic regression decision line for the entire data set.

Table 1. Accuracy of Spectroscopic Classification of Nondysplastic, Low-grade, and High-grade Dysplastic Tissue in BE

	HGD vs. LGD and NDB		LGD and HGD vs. NDB	
	Sensitivity	Specificity	Sensitivity	Specificity
Intrinsic fluorescence (IF)	100%	97%	79%	88%
Diffuse reflectance (DR)	86%	100%	79%	88%
Light scattering (LS)	100%	91%	93%	96%
Combination of IF, DR, and LS	100%	100%	93%	100%

HGD, High-grade dysplastic; LGD, low-grade dysplastic; NDB, nondysplastic Barrett's esophagus.

This analysis shows that the reduced scattering coefficient, μ_s', of Barrett's esophagus tissue changes gradually during the progression from nondysplastic, to low-grade, to high-grade dysplasia. For example, at 400 nm, the μ_s' of high-grade dysplastic tissue (1.3 ± 0.2 mm^{-1}) is lower than that of low-grade dysplastic tissue (1.8 ± 0.3 mm^{-1}), which, in turn, is lower than that of nondysplastic BE tissue (3 ± 1.6 mm^{-1}). Additionally, the wavelength dependence of μ_s' changes during the development of dysplasia. To describe these changes, a straight line is fit to $\mu_s'(\lambda)$ and the intercept at 0 nm and slope of this line are used as diagnostic parameters (Figure 7). Using logistic regression and leave-one-out cross-validation, the sensitivity and specificity for classifying tissue in accordance with histopathology are determined.

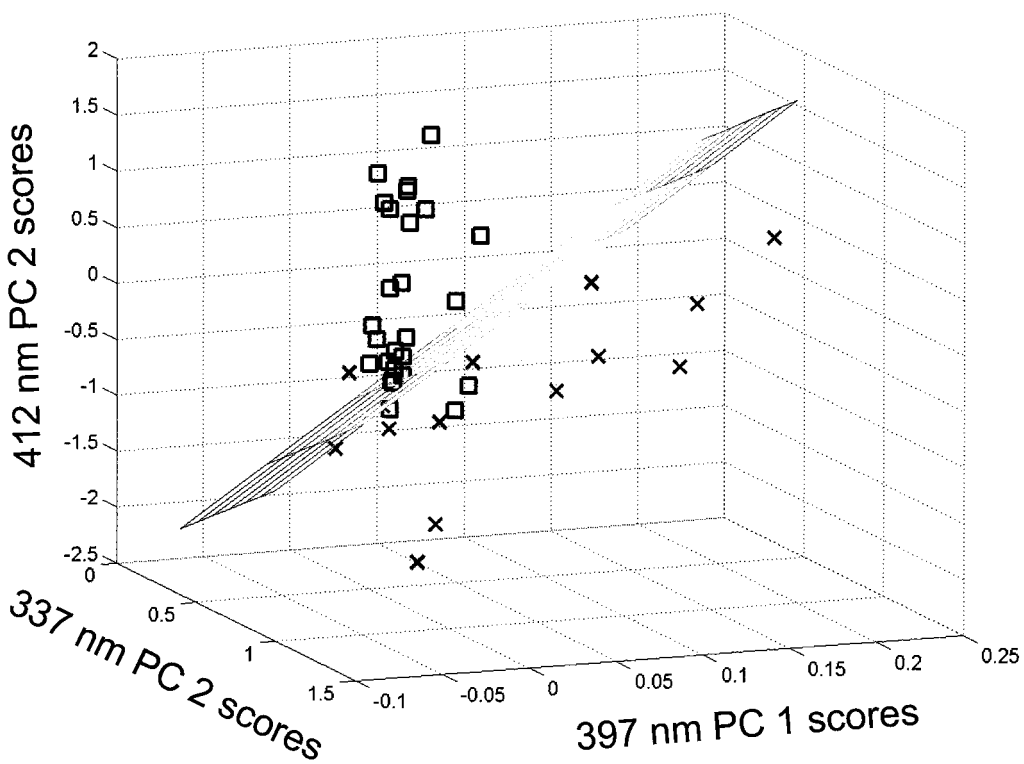

Figure 5. Scores of 3 principal components extracted from decomposition of the intrinsic fluorescence spectra excited at 337 (460–520-nm emission), 397 (600–650-nm emission), and 412 nm (360–750-nm emission) used to distinguish dysplastic (low- and high-grade; ×) from nondysplastic (□) BE sites. PC 1, first principal component; PC 2, second principal component. The logistic regression decision plane for the entire data set is also shown.

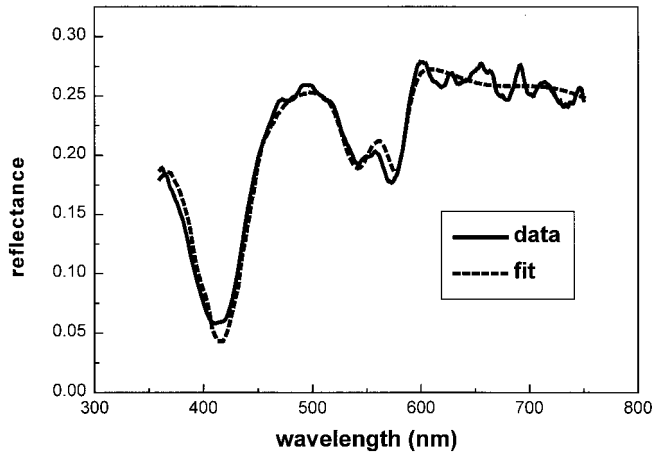

Figure 6. Reflectance spectrum of a nondysplastic BE site. *Solid line*, experimental data; *dashed line*, model fit.

This method results in slightly lower overall sensitivity and specificity values than those achieved with the intrinsic fluorescence spectra (Table 1).

Light-Scattering Spectroscopy

The reflectance spectra are further processed in a manner that allows extraction and analysis of the reflected light scattered from the epithelial cell nuclei. The results of this analysis are displayed in Figure 8. The ordinate of this figure represents the number of nuclei per square millimeter, indicative of the degree of nuclear crowding, and the abscissa represents the percentage of enlarged nuclei, defined as nuclei having a diameter >10 μm. Note that the nondysplastic samples are concentrated in the lower left-hand corner, indicating cell nuclei that are small and free of crowding. As dysplasia progresses, the data points move to the upper right, indicating nuclear enlargement and crowding, in agreement with the findings of histopathology. This technique is superior in terms of separating the dysplastic (low- and high-grade) from the nondysplastic BE sites (Table 1).

Combination of Spectroscopic Techniques for Optimal Diagnosis

The ability to characterize dysplastic and nondysplastic tissue in BE is improved by combining the information provided by each one of the spectroscopic techniques, obtained simultaneously with our system. When a spectroscopic classification is consistent with at least 2 of the 3 analysis methods, high-grade dysplasia is identified with very high sensitivity and specificity, and dysplastic tissue is distinguished from nondysplastic tissue with very high specificity, while maintaining high sensitivity (Table 1).

Discussion

Spectroscopic techniques use information contained in light signals to assess the state of biological tissue. Optical fiber technology allows spectroscopy to be applied as a diagnostic tool for a wide range of tissues that are accessible endoscopically. Indeed, the use of spectroscopy as a means of improving the physician's ability to detect precancerous (dysplastic) and early cancerous lesions is pursued actively in many organs, such as the oral cavity,[35–38] the cervix,[39,40] the lung,[41,42] the breast,[43] and the gastrointestinal tract.[6–14,44–46] Depending on the technique used, specific information can be acquired about tissue biochemical, architectural, and morphologic features. Microscopic changes in these features that occur during the progression of dysplasia may be detectable spectroscopically before the manifestation of macroscopic changes that are visible endoscopically. Additionally, spectroscopic techniques are noninvasive, allowing study of the tissue in its native state, free of

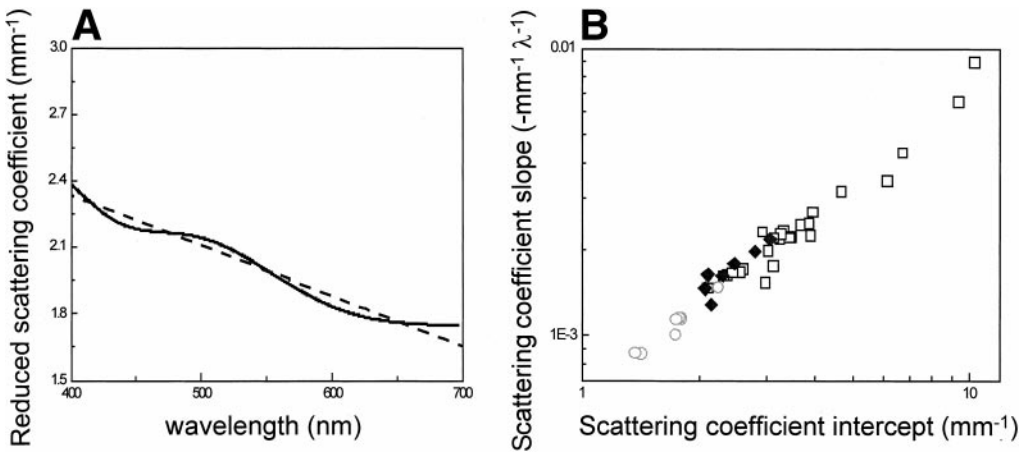

Figure 7. (*A*) Reduced scattering coefficient as a function of wavelength for a representative nondysplastic BE site (*solid line*) and corresponding linear fit (*dashed line*). (*B*) Slopes and intercepts of linear fit to the wavelength-dependent tissue reduced scattering coefficient, μ_s', for nondysplastic (□), low-grade (◆), and high-grade (○) dysplastic BE sites. A log-log scale is used to facilitate visualization of all the data points.

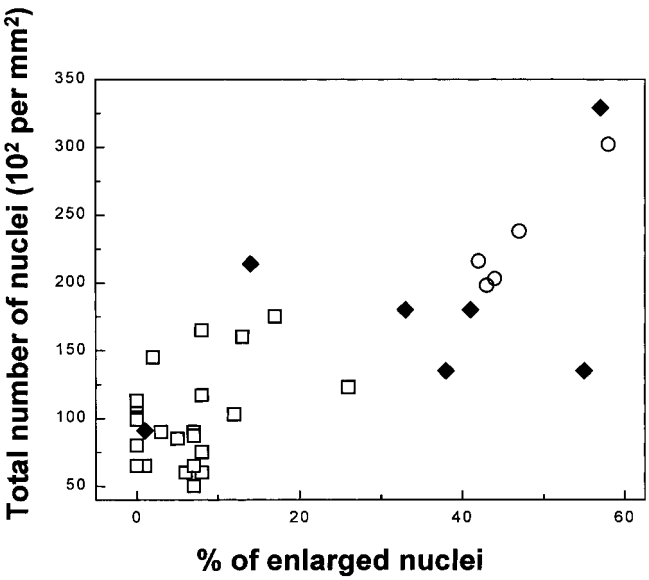

Figure 8. Total number of nuclei/mm^2 plotted as a function of percentage of enlarged nuclei (diameter >10 μm), as determined from the light-scattering model analysis. Nondysplastic BE, □; low-grade dysplasia, ◆; high-grade dysplasia, ○.

artifacts introduced by cutting and chemically processing the tissue. In principle, spectroscopic signals can be analyzed in real time, thus guiding the physician to biopsy areas that are likely to yield significant pathology or possibly allowing the physician to make an immediate decision on the type of intervention that is required for the successful treatment of the patient. Furthermore, the spectroscopic signals carried by light can be used as objective guides for assessing a particular tissue site, especially in areas in which the intra- and interobserver agreement on the classification of disease is not very good.

In this report, we show the ability of 3 different spectroscopic techniques (fluorescence, reflectance, and light scattering) to characterize biochemical and morphologic changes that occur during the progression of dysplasia in BE. We show the different types of information that can be acquired and the way this information can be used to assist the physician in classifying a particular tissue area. The accuracy of these techniques is evident from the high sensitivity and specificity with which we can distinguish not only high-grade, but also low-grade dysplastic changes (Table 1). To our knowledge, this is the first report of a study in which multiple spectroscopic techniques are combined to provide superior results for the detection of early dysplastic changes and the classification of tissue in a manner that is consistent with histopathologic findings.

Fluorescence spectroscopy is under development in many areas as a diagnostic tool. The targets of fluorescence spectroscopy consist of tissue biochemicals such as reduced nicotinamide adenine dinucleotide (NADH), flavin adenine dinucleotide, collagen, elastin, and porphyrins. Exogenous or exogenously induced chromophores that have been shown to accumulate preferentially in the diseased areas can also be used. Promising results for the detection of high-grade dysplasia using tissue autofluorescence excited at 410 nm have been obtained by Vo-Dinh et al.[6–9] The difference between the measured integrated intensity-normalized fluorescence and the mean normalized fluorescence from normal esophageal tissue was used for the diagnostic algorithm. The main spectral features that resulted in good differentiation between high-grade dysplastic and nondysplastic tissues were the presence of decreased fluorescence around 470–480 nm and increased fluorescence in the red region of the spectrum for the high-grade dysplastic tissues. However, this algorithm could not classify correctly sites with low-grade or focal high-grade dysplasia.

In this study, we obtain fluorescence spectra at 11 different excitation wavelengths between 337 and 610 nm. Thus, instead of a single fluorescence spectrum, we have an EEM. EEMs can be used to identify the excitation wavelengths at which tissue classification is optimized. Additionally, EEMs can assist in identifying the origins of the measured fluorescence signals in a more reliable manner. Nevertheless, as shown in Figures 2 and 3, these measured EEMs can be distorted significantly by tissue scattering and absorption. To eliminate artifactual changes introduced by changes in scattering or absorption, rather than by tissue biochemistry, we use the corresponding reflectance spectra, which are affected in a similar manner by scattering and absorption events. Once the distorted measured tissue fluorescence spectra are rectified using the reflectance, we observe that tissue fluorescence excited at 337 nm broadens and shifts to longer wavelengths in a very consistent manner as the tissue progresses from nondysplastic to low-grade to high-grade dysplasia (Figure 3). These spectral changes are consistent with the presence of increased NADH levels in dysplastic tissue. Our findings at 397- and 412-nm excitation are consistent with the results of Vo-Dinh et al.[6–9] with respect to the differences in the red fluorescence, which is attributed to endogenous porphyrins. The spectra corresponding to the high-grade dysplasia sites appear slightly distorted around 470 nm, even after correcting for the effects of scattering and absorption. This suggests that this difference arises as a result of biochemical changes rather than absorption changes.

To demonstrate the level of significant changes that are observed in tissue fluorescence during the development of dysplasia, we use the scores of 1 of the first 3 principal components, which collectively describe over 99% of the variance observed in the intrinsic fluorescence spectra excited at 337, 397, and 412 nm. Subsequently, we use logistic regression and leave-one-out cross-validation to estimate and validate in an unbiased manner the sensitivity and specificity with which we can distinguish (1) high-grade dysplasia from low-grade and nondysplastic tissue, and (2) dysplastic (low- and high-grade) from nondysplastic tissue. We find that when we attempt to separate high-grade dysplasia from low-grade and nondysplastic tissue, spectroscopic classification is consistent with histopathology in all but 1 case. Additionally, we can distinguish dysplastic from nondysplastic tissue with very high sensitivity and specificity.

While these initial results are very promising, our ultimate goal is to decompose the intrinsic tissue fluorescence EEMs into EEMs of specific biochemicals, and thus to correlate the observed changes with particular changes in tissue biochemistry. Such knowledge of the events that take place during the progression of dysplasia should lead to improved detection capabilities and to improved understanding of dysplasia in general.

Reflectance spectroscopy can be used not only to remove the distortions observed in the measured tissue fluorescence spectra, but also to provide very detailed and potentially useful information about morphologic and architectural features of the tissue. Specifically, we show in Figure 6 that we can describe the observed tissue reflectance spectra in terms of 2 parameters that are determined by tissue scattering and absorption. For example, changes in the concentration or the oxygen saturation of hemoglobin, the main absorber in the visible spectrum for this tissue type, will result in concomitant changes in the absorption coefficient of tissue. Alterations in the architecture of the connective tissue collagen fibers, one of the main contributors of tissue scattering in diffuse reflectance measurements,[32] will lead to a modified tissue scattering coefficient. Indeed, our analysis suggests that the scattering coefficient of tissue decreases significantly during the development of dysplasia, suggesting that changes that are not observed histopathologically are taking place within the lamina propria and submucosa before the onset of invasion. Recently, it has been shown that an increased level of cysteine and serine proteases is found in gastric and colorectal cancerous and precancerous lesions.[47] Our findings related to the decrease in the value of the scattering coefficient during the progression of dysplasia are consistent with the presence of such enzymes, which could result in a less dense collagen matrix, for instance. The change in the slope of μ_s' as a function of wavelength suggests that the mean size of the tissue scattering particles is changing. Crowding of the cells and nuclei of the epithelial layer may be responsible for this change. As shown in Table 1, we can use the observed changes in tissue scattering to classify tissue quite successfully.

Light-scattering spectroscopy is a novel technique that can be used to obtain information about the number and the size of nuclei of the epithelial cell layer. Epithelial cell nuclei are the primary targets of reflected light that is singly scattered before it is collected by our probe. The intensity and oscillations of this singly backscattered light are characteristic of the number and size of its target nuclei. We have used this technique to characterize precancerous and early cancerous changes in the colon, the oral cavity, the bladder, and BE.[14,34] We include the results of this technique for the data set of this particular study to illustrate the information that can be acquired and combined with fluorescence and reflectance spectroscopies. We find that light-scattering spectroscopy outperforms the other 2 methods in terms of its ability to separate the dysplastic from the nondysplastic BE sites.

The combination of all 3 techniques is an extremely sensitive and specific tool for the detection of dysplasia in BE and provides superior results to any 1 of the techniques alone. In this case, the spectroscopic classification is in agreement with the histopathological one for all 7 high-grade dysplastic sites and 33 non–high-grade sites. Additionally, all sites are classified correctly as dysplastic or nondysplastic, with the exception of 1 site. The observed improvement is expected because each of the techniques examines different features of tissue biochemistry and morphology that can be altered during the development of dysplastic changes. We note that in a larger data set, less than perfect agreement is to be expected.

These very promising and substantial results demonstrate the ability of spectroscopic techniques to provide useful information for disease classification in a noninvasive manner. Although each of the techniques discussed in this article shows great potential as a means of detecting dysplasia in BE, their combination should allow us to create a comprehensive picture of the biochemical and morphologic state of tissue. Specifically, decomposition of the intrinsic tissue fluorescence EEMs into EEMs of biochemicals such as NADH and collagen will provide details about tissue biochemistry. Reflectance and light scattering spectroscopy yield morphologic information

related to the connective tissue and the epithelial cell nuclei. Because this information is free from artifacts introduced by tissue excision and processing, it can help advance the understanding of the processes that lead to the progression of dysplasia. Development of software for performing data analysis using all 3 types of spectroscopic information in real time at endoscopy will allow us to test the applicability of these techniques as a guide to performing biopsies in the near future. Extension of these methods to imaging modalities will enable large tissue areas to be studied rapidly.

References

1. Antonioli D. The esophagus. In: Henson D, Alobores-Saavdera J, eds. The pathology of incipient neoplasia. Philadelphia: Saunders, 1993:64–83.
2. Van Sandick JW, van Lanschot JJB, Kuiken BW, Tytgat GNJ, Offerhaus GJA, Obertop H. Impact of endoscopic biopsy surveillance of Barrett's esophagus on pathological stage and clinical outcome of Barrett's carcinoma. Gut 1998;43:216–222.
3. Cameron AJ. Management of Barrett's esophagus. Mayo Clin Proc 1998;73:457–461.
4. Reid BJ, Haggitt RC, Rubin CE, Roth G, Surawicz CM, Van Belle G, Lewin K, Weinstein WM, Antonioli DA, Goldman H, McDonald W, Owen D. Observer variation in the diagnosis of dysplasia in Barrett's esophagus. Hum Pathol 1988;19:166–178.
5. Petras RE, Sivak MV, Rice TW. Barrett's esophagus. A review of the pathologist's role in diagnosis and management. Pathol Annual 1991;26:1–32.
6. Panjehpour M, Overholt BF, Schmidhammer JL, Farris C, Buckley PF, Vo-Dinh T. Spectroscopic diagnosis of esophageal cancer: new classification model, improved measurements system. Gastrointest Endosc 1995;41:577–581.
7. Vo-Dinh T, Panjehpour M, Overholt BF, Farris C, Buckley RP, Sneed R. In vivo diagnosis of the esophagus using differential normalized fluorescence (DNF) indices. Lasers Surg Med 1995; 16:41–47.
8. Panjehpour M, Overholt B, Vo-Dinh T, Haggitt R, Edwards D, Buckley FP. Endoscopic fluorescence detection of high-grade dysplasia in Barrett's esophagus. Gastroenterology 1996;111:93–101.
9. Vo-Dinh T, Panjehpour M, Overholt BF. Laser-induced fluorescence for esophageal cancer and dysplasia diagnosis. Ann N Y Acad Sci 1998;838:116–122.
10. Stepp H, Sroka R, Baumgartner R. Fluorescence endoscopy of gastrointestinal diseases: basic principles, techniques, and clinical experience. Endoscopy 1998;30:379–386.
11. Messmann H, Knüchel R, Bäumler W, Holstege A, Schölmerich J. Endoscopic fluorescence detection of dysplasia in patients with Barrett's esophagus, ulcerative colitis, or adenomatous polyps after 5 aminolevulinic acid-induced protoporphyrin IX sensitization. Gastrointest Endosc 1999;49:97–101.
12. Braichotte DR, Wagnières GA, Bays R, Monnier P, van den Bergh HE. Clinical pharmacokinetic studies of Photofrin by fluorescence spectroscopy in the oral cavity, the esophagus, and the bronchi. Cancer 1995;75:2768–2778.
13. Staël von Holstein C, Nilsson AMK, Andersson-Engels S, Willén R, Walther B, Svanberg K. Detection of adenocarcinoma in Barrett's oesophagus by means of laser induced fluorescence. Gut 1996;39:711–716.
14. Wallace MB, Backman V, Perelman LT, Crawford JM, Fitzmaurice M, Seiler M, Badizadegan K, Shields SJ, Itzkan I, Dasari RR, Van Dam J, Feld MS. Endoscopic detection of dysplasia in patients with Barrett's esophagus using light-scattering spectroscopy. Gastroenterology 2000;119:677–682.
15. Bouma BE, Tearney GJ, Compton CC, Nishioka NS. High-resolution imaging of the human esophagus and stomach in vivo using optical coherence tomography. Gastrointest Endosc 2000;51: 467–474.
16. Sivak MV Jr, Kobayashi K, Izatt JA, Rollins AM, Ung-Runyawee R, Chak A, Wong RC, Isenberg GA, Willis J. High-resolution endoscopic imaging of the GI tract using optical coherence tomography. Gastrointest Endosc 2000;51:474–479.
17. Pitris C, Jesser C, Boppart SA, Stamper D, Brezinski ME, Fujimoto JG. Feasibility of optical coherence tomography for high-resolution imaging of human gastrointestinal tract malignancies. J Gastroenterol 2000;35:87–92.
18. Wallace M, Van Dam J. Enhanced gastrointestinal diagnosis: light-scattering spectroscopy and optical coherence tomography. Gastrointest Endosc Clin N Am 2000;10:71–80.
19. Mayevsky A, Chance B. Repetitive patterns of metabolic changes during cortical spreading depression of the awake rat. Brain Res 1974;65:529–533.
20. Mayevsky A, Chance B. Intracellular oxidation-reduction state measured in situ by a multichannel fiber-optic surface fluorometer. Science 1982;217:537–540.
21. Renault G, Raynal E, Sinet M, Muffat-Joly M, Berthier J, Cornillault J, Godard B, Pocidalo J. In situ double-beam NADH laser fluorimetry: choice of a reference wavelength. Am J Physiol 1984; 246(Heart Circ Physiol 15):H491–H499.
22. Zângaro RA, Silveira L, Manoharan R, Zonios G, Itzkan I, Dasari RR, Van Dam J, Feld MS. Rapid multiexcitation fluorescence spectroscopy system for in vivo tissue diagnosis. Appl Optics 1996;35:5211–5219.
23. Cothren RM, Hayes GB, Kramer JR, Sacks B, Kittrell C, Feld MS. A multifiber catheter with an optical shield for laser angiosurgery. Lasers Life Sci 1986;1:1–12.
24. Wu J, Feld MS, Rava RP. Analytical model for extracting intrinsic fluorescence in turbid media. Applied Optics 1993;32:3585–3595.
25. Zhang Q, Müller MG, Wu J, Feld MS. Turbidity-free fluorescence spectroscopy of biological tissue. Optics Lett 2000;25:1451–1453.
26. Jackson JE. A user's guide to principal components. New York: Wiley, 1991.
27. Fisher L, VanBelle G. Biostatistics: a methodology for the health sciences. New York: Wiley, 1993.
28. Pagano M, Gauvreau K. Principles of biostatistics. Belmont, CA: Duxbury Press, 1993.
29. Schumacher M, Hollander N, Sauerbrei W. Resampling and cross-validation techniques: a tool to reduce bias caused by model building? Stat Med 1997;16:2813–2827.
30. Van Houwelingen JC, Le Cessie S. Predictive value of statistical models. Stat Med 1990;9:1303–1325.
31. Zonios G, Perelman LT, Backman V, Manoharan R, Fitzmaurice M, Van Dam J, Feld MS. Diffuse reflectance spectroscopy of human adenomatous colon polyps in vivo. Appl Optics 1999;38: 6628–6637.
32. Saidi IS, Jacques SL, Tittel FK. Mie and Rayleigh modeling of visible-light scattering in neonatal skin. Appl Optics 1995;34: 7410–7418.
33. Perelman LT, Backman V, Wallace M, Zonios G, Manoharan R, Nusrat A, Shields S, Seiler M, Lima C, Hamano T, Itzkan I, Van Dam J, Crawford JM, Feld MS. Observation of periodic fine structure in reflectance from biological tissue: a new technique for measuring nuclear size distribution. Phys Rev Lett 1998;80: 627–630.
34. Backman V, Wallace M, Perelman LT, Arendt JT, Gurjar R, Müller MG, Zhang Q, Zonios G, Kline E, McGillican T, Shapsay S, Valdez T, Badizadegan K, Crawford JM, Fitzmaurice M, Kabani S, Levin

HS, Seiler M, Dasari RR, Itzkan I, Van Dam J, Feld MS. Detection of preinvasive cancer cells. Nature 2000;406:35–36.
35. Inaguma M, Hashimoto K. Porphyrin-like fluorescence in oral cancer: in vivo fluorescence spectral characterization of lesions by use of a near-ultraviolet excited autofluorescence diagnosis system and separation of fluorescent extracts by capillary electrophoresis. Cancer 1999;86:2201–2211.
36. Betz CS, Mehlmann M, Rick K, Stepp H, Grevers G, Baumgartner R, Leunig A. Autofluorescence imaging and spectroscopy of normal and malignant mucosa in patients with head and neck cancer. Lasers Surg Med 1999;25:323–234.
37. Gillenwater A, Jacob R, Ganeshappa R, Kemp B, El-Naggar AK, Palmer JL, Clayman G, Mitchell MF, Richards-Kortum R. Noninvasive diagnosis of oral neoplasia based on fluorescence spectroscopy and native tissue autofluorescence. Arch Otolaryngol Head Neck Surg 1998;124:1251–1258.
38. Dhingra JK, Perrault DF, McMillan K, Rebeiz EE, Kabani S, Manoharan R, Itzkan I, Feld MS, Shapshay S. Early diagnosis of upper aerodigestive tract cancer by autofluorescence. Arch Otolaryngol Head Neck Surg 1996;122:1181–1186.
39. Mitchell MF, Cantor SB, Ramanujam N, Tortolero-Luna G, Richards-Kortum R. Fluorescence spectroscopy for diagnosis of squamous intraepithelial lesions of the cervix. Obstet Gynecol 1999; 93:462–470.
40. Ramanujam N, Mitchell MF, Mahadevan-Jansen A, Thomsen SL, Staerkel G, Malpica A, Wright T, Atkinson N, Richards-Kortum R. Cervical precancer detection using a multivariate statistical algorithm based on laser-induced fluorescence spectra at multiple excitation wavelengths. Photochem Photobiol 1996;64:720–735.
41. Hung J, Lam S, LeRiche JC, Palcic B. Autofluorescence of normal and malignant bronchial tissue. Lasers Med Surg 1991;11:99–105.
42. Lam S, MacAulay C, Hung J, LeRiche J, Profio AE, Palcic B. Detection of dysplasia and carcinoma in situ with a lung imaging fluorescence endoscope device. J Thor Cardiovasc Surg 1993; 105:1035–1040.
43. Alfano RR, Tang GC, Pradhan A, Lam W, Choy DSJ, Opher E. Fluorescence spectra from cancerous and normal human breast and lung tissues. IEEE J Quantum Electron 1987;23:1806–1811.
44. Cothren RM, Richards-Kortum R, Sivak MV, Fitzmaurice M, Rava RP, Boyce GA, Doxtader M, Blackman R, Ivanc TB, Hayes GB, Feld MS, Petras RE. Gastrointestinal tissue diagnosis by laser-induced fluorescence spectroscopy at endoscopy. Gastrointest Endosc 1990;36:105–111.
45. Schomacker KT, Frisoli JK, Compton CC, Flotte TJ, Richter JM, Deutsch TF, Nishioka NS. Ultraviolet laser-induced fluorescence of colonic polyps. Gastroenterology 1992;102:1155–1160.
46. Mycek MA, Schomacker KT, Nishioka NS. Colonic polyp differentiation using time-resolved autofluorescence spectroscopy. Gastrointest Endosc 1998;48:390–394.
47. Herszenyi L, Plebani M, Carraro P, De Paoli M, Roveroni G, Cardin R, Foschia F, Tulassay Z, Naccarato R, Farinati F. Proteases in gastrointestinal neoplastic diseases. Clin Chim Acta 2000;291: 171–187.

Received June 27, 2000. Accepted February 8, 2001.

Address requests for reprints to: Irene Georgakoudi, Ph.D., Massachusetts Institute of Technology, G.R. Harrison Spectroscopy Laboratory, 77 Massachusetts Avenue, Room 6-014, Cambridge, Massachusetts 09139. e-mail: ireneg@mit.edu; fax: (617) 253-4513.

Supported by National Institutes of Health grants P41RR02594 and CA53717, and by an NIH NRSA fellowship (to I.G.).